Robust half-metallic antiferromagnets LaAVOsO$_6$ and LaAMoYO$_6$ (A=Ca,Sr,Ba; Y=Re,Tc) from first-principles calculations

Y. K. Wang
Center for General Education, Tajen Institute of Technology, Pingtung 907, Taiwan

G. Y. Guo*
Department of Physics, National Taiwan University, Taipei 106, Taiwan
and Department of Physics, Chinese University of Hong Kong, Shatin, N. T., Hong Kong
(Received 31 August 2005; revised manuscript received 29 December 2005; published 27 February 2006)

We have theoretically designed three families of the half-metallic (HM) antiferromagnets (AFM), namely, LaAVOsO$_6$, LaAMoTcO$_6$, and LaAMoReO$_6$ (A=Ca,Sr,Ba), based on a systematic *ab initio* study of the ordered double perovskites LaABB'O$_6$ with the possible B and B' pairs from all the 3d, 4d, and 5d transition metal elements being considered. Electronic structure calculations based on first-principles density-functional theory with generalized gradient approximation for more than 60 double perovskites LaCaBB'O$_6$ have been performed using the all-electron full-potential linearized augmented-plane-wave method. The found HM-AFM state in these materials survives the full *ab initio* lattice constant and atomic position optimizations which were carried out using the frozen-core full potential projector augmented wave method. It is found that the HM-AFM properties predicted previously in some of the double perovskites would disappear after the full structural optimizations. The AFM is attributed to both the superexchange mechanism and the generalized double exchange mechanism via the $B(t_{2g})$-O$(2p_\pi)$-$B'(t_{2g})$ coupling and the latter is also believed to be the origin of the HM. Finally, in our search for the HM-AFMs, we find LaACrTcO$_6$ and LaACrReO$_6$ to be AFM insulators of an unconventional type in the sense that the two antiferromagnetic coupled ions consist of two different elements and that the two spin-resolved densities of states are no longer the same. It is hoped that our interesting predictions would stimulate further experimental searches for the HM-AFMs which have so far been unsuccessful.

DOI: 10.1103/PhysRevB.73.064424 PACS number(s): 75.10.Lp, 71.20.−b, 75.50.Ee

I. INTRODUCTION

Half-metallic (HM) ferromagnets (FM) were first discovered by de Groot *et al.*[1] based on their band structure calculations for magnetic semi-Heusler compounds NiMnSb and PtMnSb. Shortly afterwards, other magnetic materials such as Fe_3O_4 (Ref. 2) and CrO_2 (Ref. 3) were also found to be half-metals. Half-metallic materials are characterized by the coexistence of metallic behavior for one electron spin and insulating behavior for the other. Their electronic density of states is completely spin polarized at the Fermi level, and the conductivity is dominated by these metallic single-spin charge carriers. Therefore half-metallic materials offer potential technological applications such as a single-spin electron source and high-efficiency magnetic sensors.[4–6]

In this work, we search for another kind of HM materials with first-principles calculations. In a HM material, the spin magnetic moment per unit cell is quantized, i.e., an integer number times Bohr magneton (μ_B).[1,5–7] It may occur that this integer for some HM materials is zero. This situation has been called half-metallic antiferromagnetism.[6,8–10] Most properties such as full spin-polarized conduction electrons, zero spin susceptibility, and no Stoner continuum, of these HM antiferromagnets (AFM) are the same as those of the HM-FMs discussed above.[6] However, there is one important difference: a HM-AFM produces no macroscopic magnetic field. Therefore a HM-AF could support 100% spin polarized charge transport without any net magnetization. Furthermore, since there is no symmetry operation (translation plus spin flip) that connects its spin-up and spin-down bands, a HM-AFM is qualitatively different from a conventional AFM such as bcc Cr. Because of their unique properties mentioned above, HM-AFMs have recently attracted considerable attention. Furthermore, they could be used as, e.g., a probe of the spin-polarized scanning tunneling microscope without perturbing the spin character of samples. The HM-AFMs are expected to play a vital role in the future spintronic devices which utilize the spin polarization of the carriers.

The first HM-AFM was proposed by van Leuken and de Groot[8] on the basis of the Heusler compound $V_7MnFe_8Sb_7In$. Due to the complexity of this material, considerable effort has been spent to come up with other candidate materials, which may be easier to synthesize. In particular, based on extensive first-principles band structure calculations for double-perovskite-structure oxides $La_2BB'O_6$, where B and B' are transition metal ions, Pickett[11] proposed the cubic double perovskite La_2VMnO_6 to be a promising candidate for a HM-AFM. In this case, V and Mn have antiferromagnetically aligned magnetic moments and they exactly cancel each other. This finding was born out by the assumption that both Mn and V ions are trivalent and more importantly, all Mn^{3+} ions are in a low spin state of $S=1$ ($t_{2g}^3\uparrow t_{2g}^1\downarrow$). More recently, Park *et al.*[12] suggested thiospinel systems Mn(CrV)S_4 and $Fe_{0.5}Cu_{0.5}(V_{0.5}Ti_{1.5})S_4$ as possible HM-AFMs, based on their electronic structure studies. In Ref. 13, the mixed-cation double perovskites

LaA'VRuO$_6$ (A'=Ca, Sr, and Ba) were suggested to be candidates for HM-AFs. Androulakis *et al.*[14] have synthesized La_2VMnO_6 samples which, however, has a cubic, partially ordered double perovskite structure. Furthermore, it exhibits ferrimagnetic (FIM) behavior rather than antiferromagnetic, with Mn and V being trivalent and with Mn being in high spin state. Therefore, to date, there has been no successful experimental realization of the HM-AFM, though it has been speculated in Refs. 11 and 13 that ordered mixed-cation double perovskites $AA'BB'O_6$ would be promising candidates for the HM-AFM.

Motivated by the theoretical and experimental works mentioned above, we have taken a rather thorough search for HM-AFMs among the mixed-cation double perovskites LaABB'O$_6$. Unlike the previous theoretical effort,[11,13] we have not only performed electronic structure calculations for a fixed crystal structure but also carried out full structural optimizations including lattice constants and atomic position relaxations. We believe that the structural optimizations would be important. In particular, though La_2VMnO_6 was predicted to be a HM-AFM in Ref. 11, it was found to be ferrimagnetic in a partly ordered double perovskite structure.[14] We have explored a variety of pairs BB' with B and B' from 3d (V, Cr, Co, Ni), 4d (Mo, Tc, Ru, Rh), and 5d (W, Re, Os, Ir) transition metals. Fortunately, we find double perovskites LaAVOsO$_6$ and LaAMoYO$_6$ (Y=Tc,Re) to be robust HM-AFMs.

II. THEORY AND COMPUTATIONAL DETAILS

Our *ab initio* theoretical search was based on first-principles calculations within density-functional theory (DFT)[15] with the local density approximation (LDA) plus the generalized gradient corrections (GGA).[16] We used the highly accurate all-electron full-potential linearized augmented plane wave (FLAPW) method[17,18] as implemented in the WIEN2k package,[19] to calculate the total energy, electronic band structure, and magnetic properties for the materials with fixed structural parameters. The FLAPW method makes no shape approximations to the electron density or potential and retains high variational freedom in all regions, and hence it is well-suited to open crystal structures with low site-symmetries such as those considered here. The wave function, charge density, and potential were expanded in terms of the spherical harmonics inside the muffin-tin spheres. The cutoff angular momentum (L_{max}) of 10 used for the wave function and of 6 used for the charge density and potential are sufficient for accurate total-energy calculations.[19] The wave function outside the muffin-tin spheres was expanded in terms of the augmented plane waves. A large number of augmented plane waves (about 115 per atom) (i.e., $R_{mt}K_{max}$=6) were included in the present calculations. The set of basis functions was supplemented with local orbitals for additional flexibility in representing the valence V 3d states, Ru 4d states, Os 5d states, and La 4f states, as well as the semicore Ca (or Sr, Ba) 3s, 3p, La 5s, 5p, O 2s states. The muffin-tin sphere radii used are 2.5 a.u. for La and Ca (or Sr, Ba), and 2.0 a.u. for V, Ru, Os, Mo, Cr, Tc, and Re, and 1.4 a.u. for O. The improved tetrahedron method is used for the Brillouin-zone integration.[20] We used 140 k-points in the irreducible Brillouin zone wedge, which correspond to 1500 k-points in the first Brillouin-zone.

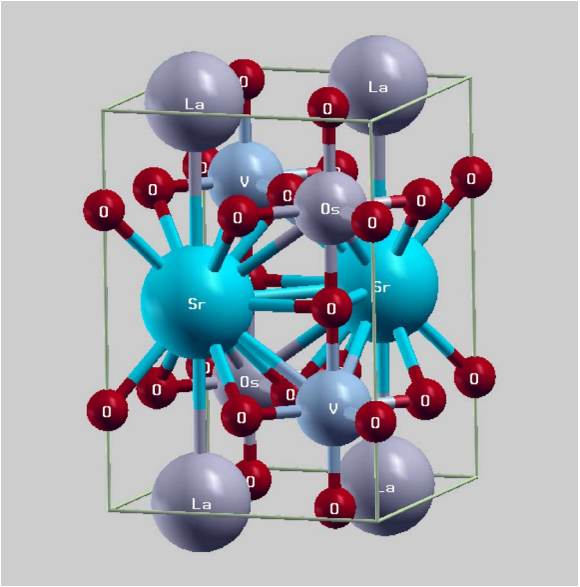

FIG. 1. (Color online) The crystal structure of an ordered double perovskite (P4/nmm).

For the structural optimization calculations to determine theoretical lattice constants and atomic positions, we used the faster frozen-core full-potential projector augmented wave method (PAW)[21] as implemented in the VASP package.[22] A cutoff energy of 450 eV for plane waves is used. A $8\times8\times6$ Monkhorst-Pack k-point grid in the Brillouin zone was used, which correspond to 30 k-points in the irreducible Brillouin-zone wedge. Their atomic positions and lattice constants were fully relaxed by a conjugate gradient technique. Theoretical equilibrium structures were obtained when the forces acting on all the atoms and the stresses were less than 0.05 eV/Å and 1.5 kBar, respectively.

III. CRYSTAL STRUCTURE AND THEORETICAL SEARCH STRATEGY

We consider LaABB'O$_6$ (A=Ca,Sr,Ba) in an ordered double perovskite structure [space group P4/nmm (No. 129)], as shown schematically in Fig. 1. This structure can be regarded as a combination of cubic LaBO$_3$ and AB'O$_3$ perovskites in a superlattice having B and B' layers stacked along the [111] direction, as in La_2CrFeO_6. Transition metal ions B and B' can couple to each other either ferromagnetically or antiferromagnetically in the [111] directions. Each B (B') ion has six B' (B) neighbors. LaBO$_3$ and AB'O$_3$ perovskites can also be stacked along the [001] direction, resulting in a double perovskite structure with the space group P4mm (No. 99), as has been considered by Park *et al.*[13] In this case, each B ion has four B ions and two B' ion neighbors, while each B' ion has four B' ions and two B ion neighbors. We have performed electronic structure calculations for LaAVRuO$_6$ and LaAVOsO$_6$ in both P4/nmm and P4mm structures. We find, however, that LaAVRuO$_6$ and

Ti	***V***	***Cr***	Mn	Fe	***Co***	***Ni***	Cu
Zr	Nb	***Mo***	***Tc***	***Ru***	***Rh***	Pd	Ag
Hf	Ta	***W***	***Re***	***Os***	***Ir***	Pt	Au

FIG. 2. (Color online) Part of the periodic table showing $3d$, $4d$, and $5d$ transition metals. Bold italic characters denote the 12 elements that have been selected as the BB' pairs for La$ABB'O_6$ in this work.

LaAVOsO_6 in the [001] stacked structure are nonmagnetic and ferrimagnetic, respectively. Furthermore, the calculated total energy for the [001] stacked structure is about 0.25–0.35 eV/f.u. higher than that of the [111] stacked structure. This shows that the [111] stacked structure is more stable and thus we will not consider the [001] stacked structure further.

The [111] stacked structure (P4/nmm) contains 20 atoms per unit cell, i.e., two chemical formula units (f.u.). It has a tetragonal symmetry with lattice constants a and c. The atomic positions of two La and two A atoms are $(1/4,3/4,0)$, $(3/4,1/4,0)$ and $(1/4,3/4,1/2)$, $(3/4,1/4,1/2)$, respectively. The atomic positions of two B and two B' atoms are $(1/4,1/4,1/4+\delta)$, $(3/4,3/4,3/4-\delta)$ and $(3/4,3/4,1/4+\delta')$, $(1/4,1/4,3/4-\delta')$, respectively. The O atoms are divided into three different types. The atomic positions of two type one and two type two O atoms are O_1: $(1/4,1/4,z_1)$, $(3/4,3/4,1-z_1)$ and O_2: $(1/4,1/4,1/2-z_2)$, $(3/4,3/4,1/2+z_2)$, respectively, while the atomic positions of eight type three O atoms are O_3: $(1/2-x,1/2-x,1/4-z_3)$, $(x,x,1/4-z_3)$, $(x,1/2-x,1/4-z_3)$, $(1/2-x,x,1/4-z_3)$, $(1/2+x,1-x,3/4+z_3)$, $(1-x,1/2+x,3/4+z_3)$, $(1-x,1-x,3/4+z_3)$, $(1/2+x,1/2+x,3/4+z_3)$. Therefore, in this structure, apart from lattice constants a and c, there are six more parameters to optimize, namely, δ, δ', x, z_1, z_2, and z_3.

For the chemical formula La$ABB'O_6$, B and B' can be an any pair from the 24 transition metal elements, as shown in Fig. 2, and A is one of the three alkali earth elements Ca, Sr, and Ba. Therefore, although we have settled down on the ordered double perovskite structure, there are still $3\times C_2^{24}=828$ possible compounds to consider. This is an impossible task. Nevertheless, our preliminary calculations and also the existing literature tell us that Ti, Cu, Zr, Nb, Pd, Ag, Hf, Ta, Pt, and Au in the double perovskite structure are usually not magnetic and thus they can be excluded from our further consideration. Furthermore, we note that in the double perovskite structure, Mn and Fe are almost always in a high spin state (see, e.g., Refs. 7, 9, and 12). Consequently, it is not possible to find a high spin state element from the remaining 12 elements to match Mn and Fe, and hence Mn and Fe are excluded from further consideration too. Therefore, in our first stage of search for HM-AFs, we consider all the possible BB' pairs from only the 12 transition metal elements as denoted by bold italic characters in Fig. 2. Furthermore, we initially confine ourselves to A=Ca. Therefore, in our first stage of search, we have performed self-consistent electronic structure calculations only for 66 ($c_2^{12}=66$) La$CaBB'O_6$ compounds in the ordered double perovskite structure with fixed lattice constants a=5.492 Å, $c=\sqrt{2}a$ taken from Ref. 13. When we find any La$CaBB'O_6$ to be a HM-AFM, we replace Ca with Sr and Ba and perform further self-consistent electronic structure calculations.

Fortunately, we find from our electronic structure calculations for 66 La$CaBB'O_6$ compounds, that six B and B' pairs, namely, VRu, VOs, MoTc, MoRe, NiTc, and NiRe, would give rise to HM-AF La$CaBB'O_6$ compounds. We note that previously, Park *et al.*[13] theoretically predicted LaAVRuO_6 to be HM-AFMs. However, we performed both volume and atomic position optimization calculations for these systems and found, unfortunately, that the HM-AFM properties predicted in Ref. 13 disappear. This perhaps explains why the attempt to synthesize the HM-AFM LaAVRuO_6 by Liu *et al.*[24] was unsuccessful. Therefore, in our second stage of search, we carried out full lattice constant and atomic position relaxation calculations for all the possible HM-AFM La$ABB'O_6$ compounds found in the first stage of search. We find fortunately that among the possible HM-AFM La$ABB'O_6$ compounds, LaAVOsO_6, LaAMoTcO_6, and LaAMoReO_6 stay as the stable HM-AFMs.

IV. RESULTS AND DISCUSSION

A. Half-metallic antiferromagnets from the initial search

In the first round of search for the HM-AFMs, we have performed *ab initio* electronic structure calculations for 66 La$CaBB'O_6$ compounds in the ideal P4/nmm structure (i.e., $\delta=\delta'=x=z_1=z_2=z_3=0$) with the lattice constants a =5.492 Å, $c=\sqrt{2}a$ taken from Ref. 13, as mentioned before. Remarkably, we found La$CaVYO_6$, La$CaMoY'O_6$, and La$CaNiY'O_6$ (Y=Ru, OS; Y'=Tc, Re) to be HM-AFMs. We then replaced Ca in these compounds with either Sr or Ba and performed further electronic structure calculations. We found again that the resultant compounds are HM-AFMs. This result could be expected because A-site atoms in ABO_3 perovskite are known to behave like a carrier reservoir and a volume conserver. The interaction between an A atom and its neighboring atoms is usually very weak such that many ABO_3's with different A's, have similar electronic properties.

In the ionic picture, the atoms in the ordered double perovskites have the nominal valence states as $La^{3+}A^{2+}(BB')^{7+}O_6^{2-}$. Therefore in, e.g., La$AVRuO_6$, the transition metal atoms B and B' can have valence configurations of $V^{3+}(3d^2)$ and $Ru^{4+}(4d^4)$, and the antiferromagnetic coupling of the high spin V^{3+} ($t_{2g}^2\uparrow$, S=1) and the low spin Ru^{4+} ($t_{2g}^3\uparrow t_{2g}^1\downarrow$, S=1) states would give rise to a zero total magnetic moment, i.e., an AFM state, Alternatively, the transition metal atoms B and B' can have valence configurations of $V^{4+}(3d^1)$ and $Ru^{3+}(4d^5)$, and the antiferromagnetic coupling of the spin V^{4+} ($t_{2g}^1\uparrow$, S=1/2) and the low spin Ru^{3+} ($t_{2g}^3\uparrow t_{2g}^2\downarrow$, S=1/2) states. Of course, in the real materials, the above simple ionic model would be modified because of hybridization between V $3d$ and O $2p$ orbitals and also between Ru $4d$ and O $2p$ orbitals. The calculated total and orbital-decomposed density of states (DOS) of LaSrVRuO_6 in the AFM state are shown in Fig. 3. Clearly, LaSrVRuO_6 is half-metallic with a band gap of about 0.8 eV on the spin-up

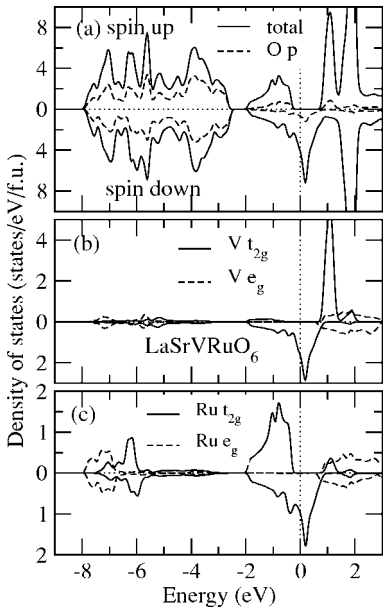

FIG. 3. Total and orbital-decomposed density of states of $LaSrVRuO_6$ in the ideal P4/*nmm* structure (no atomic position relaxation, see text and Table I).

channel. The electronic structure consists of the O $2p$ dominant lower valence band between 2.5 and 8.0 eV below the Fermi level (E_F), the spin-up Ru t_{2g} dominant upper valence band between 0.3 and 2.0 eV below E_F and spin-down Ru t_{2g}-V t_{2g} hybridized conduction band between 2.0 eV below E_F and ~1.0 eV above E_F as well as the spin-up V t_{2g} dominant, Ru e_g dominant, and V e_g dominant upper conduction bands about 0.8 eV above E_F (see Fig. 3). The calculated DOS spectra are very similar to the ones reported in Ref. 13. Our calculated occupation numbers are 0.72 e (spin-up) and 1.68 e (spin-down) at the V-site, and 2.72 e (spin-up) and 1.98 e (spin-down) on the Ru-site. Therefore the calculated charge configurations are $V^{2.6+}(3d^{2.4})$ and $Ru^{3.3+}(4d^{4.7})$, suggesting that the valence configurations of V^{3+}/Ru^{4+} and V^{4+}/Ru^{3+} are perhaps nearly degenerate and hence highly mixed, as pointed out before.[13] This notion is further supported by the fact that the calculated local spin magnetic moments of V and Ru are not integer numbers of 2 or 1 but less than 1.0 (see Table I).

Similarly, we can understand the formation of the AFM state in the other HM-AFM compounds in the ionic picture. As for LaAVRuO$_6$, in LaAVOsO$_6$, the transition metal atoms B and B' can have valence configurations of $V^{3+}(3d^2)$ and $Os^{4+}(5d^4)$, and the antiferromagnetic coupling of the high spin V^{3+} ($t_{2g}^2\uparrow$, S=1) and the low spin Os^{4+} ($t_{2g}^3\uparrow t_{2g}^1\downarrow$, S=1) states would give rise to a zero total magnetic moment. In LaAMoTc(Re)O$_6$, the transition metal atoms B and B' may have valence configurations of $Mo^{3+}(4d^3)$ and $Tc^{4+}(4d^3)$ [$Re^{4+}(5d^3)$] with the antiferromagnetic coupling of the low spin Mo^{3+} ($t_{2g}^2\uparrow t_{2g}^1\downarrow$, S=1/2) and the low spin Tc(Re)$^{4\pm}$ ($t_{2g}^2\uparrow t_{2g}^1\downarrow$, S=1/2) states. In La$A$NiTc(Re)O$_6$, the transition metal atoms B and B' may have valence configurations of $Ni^{2+}(3d^8)$ and $Tc^{5+}(4d^2)$ [$Re^{5+}(5d^2)$] with the antiferromagnetic coupling of the high spin Ni^{2+} ($t_{2g}^3\uparrow t_{2g}^3\downarrow e_g^2\uparrow$, S=1) and the high spin Tc(Re)$^{5+}$ ($t_{2g}^2\uparrow t_{2g}^0\downarrow$, S=1) states.

To see whether the HM-AFM is the stable state in these six compounds, we performed the FM electronic structure calculations. Unfortunately, we find that the total energy of the HM-AFM state in LaANiY'O$_6$ (Y'=Tc,Re) is substantially higher than that of the FM state, by 0.19 and 0.18 eV/formula unit (f.u.), respectively. This suggests that the HM-AFM state in these two systems is not stable and hence we will not consider them further. We then performed volume relaxation calculations for LaAVYO$_6$ and LaAMoY'O$_6$ (A=Ca,Sr,Ba; Y=Ru,Os; Y'=Tc,Re) starting with both the FM and AFM states. We find all these systems to remain as a stable HM-AFM after the volume relaxation. The calculated electronic and magnetic properties of these four families of the double perovskites are listed in Tables I–IV, respectively.

Tables I–IV show clearly that the total energy of the HM-AFM state in these four families of the double perovskites is significantly lower than that of the corresponding FM or non

TABLE I. Calculated physical properties of LaAVRuO$_6$ in the ideal P4/*nmm* structure ($\delta=\delta'=x=z_1=z_2=z_3=0$).

A=		Ca		Sr		Ba	
Magnetic states		FM/NM	AF	FM/NM	AF	FM/NM	AF
a (Å)		5.510	5.517	5.545	5.553	5.604	5.612
c/a		$\sqrt{2}$		$\sqrt{2}$		$\sqrt{2}$	
V (Å^3/f.u.)		118.31	118.72	120.57	121.05	124.44	125.00
m_V (μ_B)		0.039	−0.949	0.017	−0.967	0.006	−0.992
m_{Ru} (μ_B)		0.074	0.730	0.028	0.738	0.016	0.744
m_t (μ_B/f.u.)		0.165	0.0	0.065	0.0	0.033	0.0
N (E_F)	↑	2.563	0.0	2.575	0.0	2.358	0.0
(states/eV/f.u.)	↓	2.491	4.064	2.640	4.205	2.460	4.414
gap (eV)	↑		0.74		0.79		0.79
ΔE^{AF-FM} (eV/f.u.)		−0.102		−0.103		−0.090	

TABLE II. Calculated physical properties of LaAVOsO$_6$ in the ideal P4/nmm structure ($\delta=\delta'=x=z_1=z_2=z_3=0$).

A=		Ca		Sr		Ba	
Magnetic states		FM/NM	AF	FM/NM	AF	FM/NM	AF
a (Å)		5.522	5.546	5.557	5.577	5.607	5.635
c/a		$\sqrt{2}$		$\sqrt{2}$		$\sqrt{2}$	
V (Å^3/f.u.)		119.05	120.61	121.36	122.67	124.62	126.53
m_{V} (μ_B)		0.0	−1.254	0.0	−1.274	0.0	−1.305
m_{Os} (μ_B)		0.0	0.890	0.0	0.899	0.0	0.910
m_t (μ_B/f.u.)		0.0	0.0	0.0	0.0	0.0	0.0
N (E_F)	↑	3.420	0.0	3.462	0.0	2.527	0.0
(states/eV/f.u.)	↓	3.420	3.798	3.462	3.883	2.527	4.023
gap (eV)	↑		0.82		0.87		0.98
ΔE^{AF-FM} (eV/f.u.)		−0.231		−0.236		−0.237	

TABLE III. Calculated physical properties of LaAMoTcO$_6$ in the ideal P4/nmm structure ($\delta=\delta'=x=z_1=z_2=z_3=0$).

A=		Ca		Sr		Ba	
Magnetic states		FM/NM	AF	FM/NM	AF	FM/NM	AF
a (Å)		5.629	5.640	5.657	5.667	5.699	5.717
c/a		$\sqrt{2}$		$\sqrt{2}$		$\sqrt{2}$	
V (Å^3/f.u.)		126.13	126.87	127.99	128.66	130.91	132.16
m_{Mo} (μ_B)		0.0	−1.007	0.0	−1.030	0.0	−1.064
m_{Tc} (μ_B)		0.0	1.112	0.0	1.133	0.0	1.164
m_t (μ_B/f.u.)		0.0	0.0	0.0	0.0	0.0	0.0
N (E_F)	↑	3.168	0.0	3.225	0.0	3.321	0.0
(states/eV/f.u.)	↓	3.168	3.160	3.225	3.184	3.321	3.271
gap (eV)	↑		0.44		0.49		0.60
ΔE^{AF-FM} (eV/f.u.)		−0.146		−0.159		−0.171	

TABLE IV. Calculated physical properties of LaAMoReO$_6$ in the ideal P4/nmm structure ($\delta=\delta'=x=z_1=z_2=z_3=0$).

A=		Ca		Sr		Ba	
Magnetic states		FM/NM	AF	FM/NM	AF	FM/NM	AF
a (Å)		5.640	5.656	5.669	5.687	5.739	5.739
c/a		$\sqrt{2}$		$\sqrt{2}$		$\sqrt{2}$	
V (Å^3/f.u.)		126.89	127.93	128.85	130.06	133.67	133.64
m_{Mo} (μ_B)		0.0	−1.138	0.0	−1.175	0.0	−1.210
m_{Re} (μ_B)		0.0	1.100	0.0	1.133	0.0	1.161
m_t (μ_B/f.u.)		0.0	0.0	0.0	0.0	0.0	0.0
N (E_F)	↑	2.925	0.0	3.003	0.0	3.175	0.0
(states/eV/f.u.)	↓	2.925	2.190	3.003	1.853	3.175	1.423
gap (eV)	↑		0.16		0.27		0.35
ΔE^{AF-FM} (eV/f.u.)		−0.148		−0.172		−0.214	

TABLE V. Theoretical structural parameters and stability of La$ABB'O_6$ in the HM-AFM as well as FM and NM states. The lattice constant a is in units of Å.

A=	Ca		Sr		Ba	
Magnetic states	FM/NM	AF	FM/NM	AF	FM/NM	AF
			(a) La$AVOsO_6$			
a (c/a)	5.538 (1.401)	5.541 (1.405)	5.585 (1.395)	5.580 (1.402)	5.652 (1.385)	5.647 (1.396)
$\delta(\delta')$ (10^{-2})	0.76 (0.39)	0.71 (0.22)	0.46 (0.33)	0.39 (0.14)	−0.09 (−0.16)	−0.03 (−0.13)
$x(z_1)$ (10^{-2})	0.60 (0.42)	0.44 (0.46)	0.60 (0.35)	0.42 (0.34)	0.56 (0.22)	0.38 (0.22)
$z_2(z_3)$ (10^{-2})	0.79 (0.59)	0.52 (0.62)	0.98 (1.14)	0.70 (1.18)	1.34 (2.07)	0.90 (1.88)
V (Å^3)	119.06	119.50	121.53	121.83	125.04	125.67
ΔE^{AF-FM} (eV/f.u.)	−0.104		−0.102		−0.099	
			(b) La$AMoTcO_6$			
a (c/a)	5.643 (1.408)	5.656 (1.408)	5.679 (1.404)	5.689 (1.406)	5.740 (1.392)	5.747 (1.399)
$\delta(\delta')$ (10^{-2})	0.49 (0.08)	0.47 (0.07)	0.14 (−0.01)	0.15 (−0.11)	−0.34 (0.06)	−0.19 (−0.25)
$x(z_1)$ (10^{-2})	0.17 (0.26)	0.67 (0.16)	0.20 (0.15)	0.02 (0.07)	0.24 (−0.10)	0.02 (−0.02)
$z_2(z_3)$ (10^{-2})	0.07 (0.58)	−0.10 (0.03)	0.26 (1.17)	0.01 (1.36)	0.62 (1.93)	0.16 (1.98)
V (Å^3)	126.50	127.35	128.54	129.41	131.64	132.77
ΔE^{AF-FM} (eV/f.u.)	−0.135		−0.149		−0.163	
			(c) La$AMoReO_6$			
a (c/a)	5.651 (1.409)	5.671 (1.408)	5.687 (1.408)	5.703 (1.409)	5.749 (1.393)	5.756 (1.404)
$\delta(\delta')$ (10^{-2})	0.40 (0.17)	0.38 (0.14)	0.20 (0.03)	0.09 (−0.07)	−0.14 (−0.18)	−0.14 (−0.28)
$x(z_1)$ (10^{-2})	−0.08 (−0.03)	−0.18 (−0.07)	−0.08 (−0.05)	−0.18 (−0.11)	−0.06 (−0.09)	−0.21 (−0.13)
$z_2(z_3)$ (10^{-2})	−0.13 (0.30)	−0.28 (0.57)	−0.10 (0.86)	−0.25 (1.09)	−0.04 (1.80)	−0.27 (1.94)
V (Å^3)	127.15	128.45	129.45	130.68	132.33	133.81
ΔE^{AF-FM} (eV/f.u.)	−0.182		−0.229		−0.271	

magnetic (NM) state. The energy difference is larger than 0.1 eV/f.u. and can be as large as ~0.24 eV/f.u., e.g., in $LaBaVOsO_6$ (Table II). The insulating gap in the spin-up band structure is rather large and can be up to 1.0 eV as in $LaBaVOsO_6$ (Table II). It is also interesting to note that no strong FM solution can be stabilized in all four families of the compounds, and hence these compounds have either a weak FM or NM metastable state (Tables I–IV). Nonetheless, the local magnetic moments in the HM-AFM state are not large either, all being in the order of 1.0 μ_B/atom.

B. Effects of structural optimization

In our second stage of search, we carried out full structural optimization (i.e., both lattice constant and atomic position relaxations) calculations for all the possible HM-AFM La$ABB'O_6$ compounds described in the previous section. Interestingly, we find that La$AVOsO_6$, La$AMoTcO_6$, and La$AMoReO_6$ (A=Ca, Sr, and Ba) remain to be the stable HM-AFMs, although La$AVRuO_6$ become nonmagnetic after the full structural optimization. The equilibrium lattice constants and atomic positions as well as the stability of the HM-AFM of these three families of the double perovskites are listed in Table V. Clearly, the HM-AFM state is stable over the FM or NM state in these compounds, and the size of the energy difference between the HM-AFM and FM/NM states is similar to the one before the full structural optimization (see Tables I–IV). The full structural optimization further lowers the total energy of these compounds rather significantly. The most pronounced decrease in the total energy occurs in the Ba-based double perovskites. For example, the decrease is about 0.2 to 0.3 eV/f.u. for $LaBaMoYO_6$ (Y=Tc,Re) and about 0.3 to 0.4 eV/f.u. for $LaBaVOsO_6$. This may be attributed to the fact that the ionic radius of Ba is significantly larger than that of Ca. This notion is further supported by the fact that the equilibrium unit cell volume increases as one replaces Ca with Sr and then with Ba (see Table V). The decrease in the total energy become smaller as one moves from Ba through Sr to Ca. The decrease in the total energy is about 0.1–0.15 eV/f.u. for $LaSrMoYO_6$ and about 0.05–0.1 eV/f.u. for $LaCaMoYO_6$ (Y=Tc,Re).

The shape (i.e., the c/a ratio) of the unit cell for the ordered double perovskites in the HM-AFM state does not change much after the full structural optimization (Table V). In particular, the deviation of the c/a for La$CaBB'O_6$ from the ideal value of $\sqrt{2}$ is less than 1%. This is because La and Ca have rather similar atomic radii of 3.92 and 4.12 a.u.,[25] respectively. The deviation increases very slightly as Ca is replaced by Sr and Ba, and the largest deviation of about 1.3% occurs in $LaBaVOsO_6$. Sr and Ba have larger atomic radii of 4.49 and 4.65, respectively. However, the internal atomic displacements after the structural optimization are rather pronounced. For example, the contraction (expansion) of the in-plane B-O (B'-O) bond length of the BO_6 ($B'O_6$) octohedra which is described by the parameter x, can be as large as 2.7% (or 0.038 Å) in $LaCaMoTcO_6$. The in-plane

TABLE VI. Theoretical structural parameters of LaAVRuO$_6$.

A= Magnetic state	Ca NM	Sr NM	Ba NM
a (Å)	5.517	5.559	5.629
c/a	1.409	1.403	1.393
$\delta(\delta')$ (10^{-2})	0.90 (0.40)	0.36 (0.36)	−0.29 (0.23)
$x(z_1)$ (10^{-2})	0.78 (0.52)	0.78 (0.38)	0.78 (0.24)
$z_2(z_3)$ (10^{-2})	0.91 (0.57)	1.25 (1.19)	1.70 (2.06)
V (Å^3/f.u.)	118.26	120.46	124.26

B-O-B' bond bending which is described by the parameters z_3, δ, and δ', is also rather significant. In particular, the B-O-B' bond bending can be as large as 8° (i.e., the angle of the B-O-B' bond is about 172°) in LaBaVOsO$_6$. A similar amount of the bond bending occurs in LaBaMoTcO$_6$ and LaBaMoReO$_6$. This may be attributed to the fact that the atomic radius of Ba is considerably larger than that of La. This bond bending becomes smaller when Ba is replaced by Sr and Ca. Another significant atomic displacement is the contraction (expansion) of the apical B-O (B'-O) bond of the BO_6 ($B'O_6$) octohedra which is described by the parameters z_1, z_2, δ, and δ'. For example, the contraction of the V-O$_2$ bond length is about 4.3%. Interestingly, this displacement of the apical O atoms is asymmetrical. Indeed, the V-O$_1$ bond is elongated slightly, i.e., expands by 0.21%.

Obviously, the full structural optimization has the largest effects on LaAVRuO$_6$ in which both the HM-AF and FM states disappear and the systems become nonmagnetic after the structural optimization, as mentioned before. The lowering of the total energy due to the structural optimization is the largest among the four families of the HM-AFM candidates found in our first stage of search, varying from 0.4 to 0.8 eV/f.u. Likewise, the contraction of the VO_6 octahedra and the expansion of the RuO_6 octahedra during the structural optimization are also the largest (see Tables V and VI). For example, the contraction (expansion) of the V-O (Ru-O) bond on the xy plane is about 3.0% and that of the apical V-O$_2$ bond is as large as 6.4%. Furthermore, the B-O-B' bond bending is around 7° in all three LaAVRuO$_6$ compounds. It is therefore conceivable that the weak AFM and FM state of LaAVRuO$_6$ found in the ideal P4/nmm structure could not sustain such large structural distortions and both of them become nonmagnetic.

Why the magnetic states disappear in LaAVRuO$_6$ after the full structural optimization can perhaps be best understood by examining their electronic structures. Figure 4 shows the total and orbital-decomposed densities of states of LaSrVRuO$_6$ in the fully optimized structure. They are similar to the ones for LaSrVRuO$_6$ in the ideal P4/nmm structure displayed in Fig. 3, except that there are not spin-polarized anymore. The electronic structure consists of the O 2p dominant lower valence band between 2.7 and 7.7 eV below E_F, the Ru t_{2g} dominant upper valence band between 0.0 and 1.9 eV below E_F, and V t_{2g} dominant lower conduction band between 0.0 eV and ~1.0 eV above E_F as well as the V t_{2g}/Ru e_g dominant upper conduction bands about 0.5 eV above E_F (see Fig. 4). The most striking feature is the pseudogap at E_F and LaSrVRuO$_6$ is a semimetal with a low DOS of 0.3 states/eV/spin/f.u. at E_F. It is clear that because of the pseudogap at E_F, LaAVRuO$_6$ are now stable against magnetic instabilities and therefore the systems stay in the nonmagnetic state.[26,27] In the nonmagnetic band structures of LaAVOsO$_6$, LaAMoTcO$_6$, and LaAMoReO$_6$, there is no such pseudogap at E_F and hence they retain the HM-AFM state after the full structural optimization.

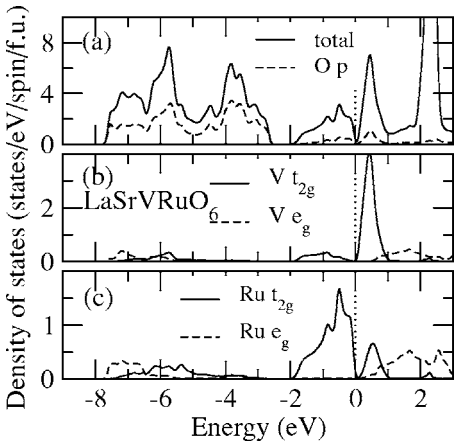

FIG. 4. Total and orbital-decomposed density of states of LaSrVRuO$_6$ in the theoretically determined P4/nmm structure (full structural optimization, see text).

C. Electronic structure and magnetic properties

The calculated electronic and magnetic properties of robust HM-AFM LaABB'O$_6$ are listed in Table VII. Clearly, all three families of LaAVOsO$_6$, LaAMoTcO$_6$, and LaAMoReO$_6$ (A=Ca,Sr,Ba) are HM-AFMs with an insulating gap in the spin-up channel. The spin-down density of states at E_F is rather large in LaAVOsO$_6$ and LaAMoTcO$_6$, although it is rather small in LaAMoReO$_6$. The insulating gap in the spin-up channel is also rather large (0.5–1.0 eV) in LaAVOsO$_6$ and LaAMoTcO$_6$ but relatively small (within 0.5 eV) in LaAMoReO$_6$. The calculated local spin magnetic moments in all the double perovskites are not large and in the order of 1.0 μ_B/atom. This seems to be consistent with the simple ionic picture described in Sec. IV A in the case of LaAMoTc(Re)O$_6$ but at variance with it in the case of LaAVOsO$_6$. The deviation from the simple ionic model is more apparent in terms of the calculated occupation numbers of the transition metal d orbitals. For example, in LaSrVOsO$_6$, the calculated occupation numbers are 0.72 e (spin-up) and 1.72 e (spin-down) at the V-site, and 2.40 e (spin-up) and 1.69 e (spin-down) on the Os-site, giving rise to a charge configuration of $V^{2.6+}(3d^{2.4})$ and $Os^{3.9+}(4d^{4.1})$. In LaSrMoTcO$_6$, the calculated occupation numbers are 0.74 e (spin-up) and 1.82 e (spin-down) at the Mo-site, and 2.40 e (spin-up) and 1.23 e (spin-down) on the Tc-site, resulting in a charge configuration of $Mo^{3.4+}(3d^{2.6})$ and $Tc^{3.4+}(4d^{3.6})$. In LaSrMoReO$_6$, the calculated occupation numbers are 0.68 e (spin-up) and 1.94 e (spin-down) at the Mo-site, and 2.14 e (spin-up) and 0.95 e (spin-down) on the Re-site, resulting in

TABLE VII. Calculated magnetic and electronic properties of LaAXYO$_6$ in theoretically determined P4/nmm structure using GGA.

A=		Ca		Sr		Ba	
Magnetic states		FM/NM	AF	FM/NM	AF	FM/NM	AF
			(a) LaAVOsO$_6$				
m_V (μ_B)		0.007	−0.985	0.007	−1.014	0.0	−1.057
m_{Os} (μ_B)		0.070	0.699	0.060	0.731	0.0	0.734
m_t (μ_B/f.u.)		0.131	0.0	0.085	0.0	0.0	0.0
N (E_F)	↑	2.321	0.0	2.006	0.0	1.909	0.0
(states/eV/f.u.)	↓	2.520	3.870	2.478	4.098	1.909	4.434
gap (eV)	↑		0.65		0.74		0.82
			(b) LaAMoTcO$_6$				
m_{Mo} (μ_B)		0.0	−1.029	0.0	−1.088	0.169	−1.128
m_{Tc} (μ_B)		0.0	1.125	0.0	1.176	0.120	1.213
m_t (μ_B/f.u.)		0.0	0.0	0.0	0.0	0.463	0.0
N (E_F)	↑	3.192	0.0	3.206	0.0	3.067	0.0
(states/eV/f.u.)	↓	3.192	3.210	3.206	3.106	2.572	3.003
gap (eV)	↑		0.52		0.68		0.79
			(c) LaAMoReO$_6$				
m_{Mo} (μ_B)		0.0	−1.226	0.0	−1.264	0.0	−1.301
m_{Re} (μ_B)		0.0	1.168	0.0	1.199	0.0	1.230
m_t (μ_B/f.u.)		0.0	0.0	0.0	0.0	0.0	0.0
N (E_F)	↑	2.947	0.0	3.086	0.0	3.333	0.0
(states/eV/f.u.)	↓	2.947	1.134	3.086	0.594	3.333	0.175
gap (eV)	↑		0.25		0.35		0.49

a charge configuration of $Mo^{3.4+}$ ($3d^{2.6}$) and $Re^{3.9+}$ ($5d^{3.1}$).

The total and orbital-decomposed DOS spectra of robust HM-AFM LaSrVOsO$_6$, LaSrMoTcO$_6$, and LaSrMoReO$_6$ are shown in Figs. 5–7, respectively. As mentioned before, when Sr is replaced by either Ca or Ba, the electronic structures of the resultant double perovskites are very similar to that of the corresponding Sr-based double perovskite, and therefore they are not shown here. Comparison of Fig. 5 with Fig. 3 shows that the electronic structure of LaSrVOsO$_6$ is very similar to that of LaSrVRuO$_6$ in the hypothetical HM-AFM state, with Os 5d playing the role of Ru 4d. Therefore, as for LaSrVRuO$_6$ in the AFM state, the electronic structure of LaSrVOsO$_6$ consists of the O 2p dominant lower valence band between 3.0 and 8.4 eV below E_F, the spin-up Os t_{2g} dominant upper valence band between 0.2 and 2.0 eV below E_F, and spin-down Os t_{2g}-V t_{2g} hybridized conduction band between 2.0 eV below E_F and ~1.0 eV above E_F as well as the spin-up V t_{2g} dominant, Os e_g dominant, and V e_g dominant upper conduction bands about 0.8 eV above E_F (see Fig. 5). LaSrVOsO$_6$ is half-metallic with a band gap of about 0.8 eV on the spin-up channel. Figure 5 shows that the lower valence band contains rather discernible contributions from transition metal B and B' d orbitals especially Os 5d in the lower part of the band because of the hybridization between O p and B (B') d orbitals. This rather strong O p-B (B') d hybridization pushes the V (Os) e_g dominant band above the V (Os) t_{2g} dominant band, as shown in Fig. 5, resulting in a crystal field splitting of the t_{2g} and e_g bands of about 2.0 eV

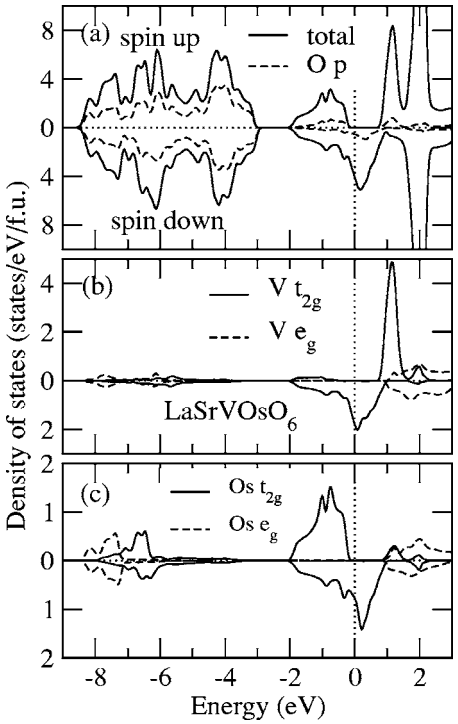

FIG. 5. Total and orbital-decomposed density of states of LaSrVOsO$_6$ in the theoretically determined P4/nmm structure (full structural optimization, see text).

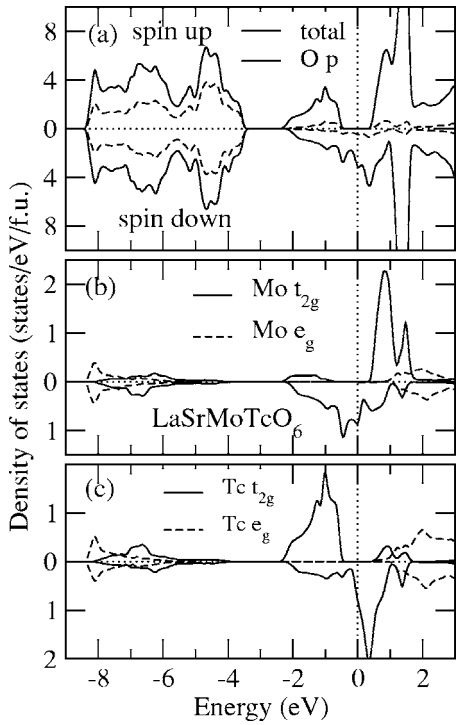

FIG. 6. Total and orbital-decomposed density of states of $LaSrMoTcO_6$ in the theoretically determined P4/*nmm* structure (full structural optimization, see text).

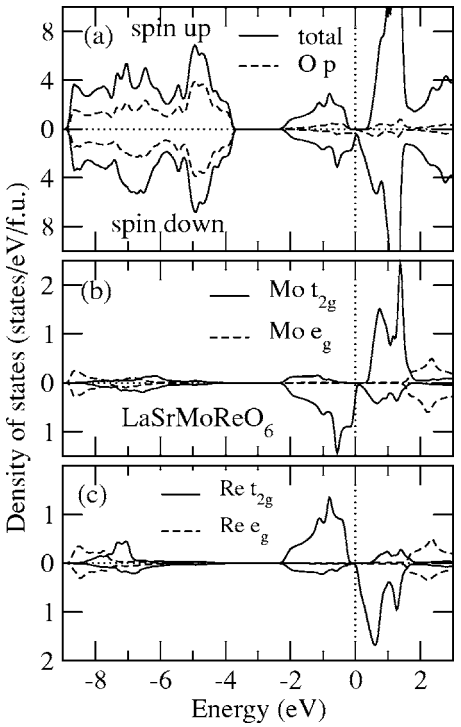

FIG. 7. Total and orbital-decomposed density of states of $LaSrMoReO_6$ in the theoretically determined P4/*nmm* structure (full structural optimization, see text).

for the VO_6 octahedron and of a slightly larger value for the OsO_6 octahedron. This B d-O p-B' d σ-bonding is the well-known superexchange coupling between the B and B' ions and gives rise to the AFM exchange interaction between the B and B' ions. However, in the conventional superexchange-type AFM insulators such as NiO, the majority (minority) spin d orbitals of each transition metal ion are separated by a large superexchange energy gap from the minority (majority) spin d orbitals of its nearest-neighbor transition metal ions. In contrast, the majority spin V t_{2g} and minority spin Os t_{2g} orbitals in $LaSrVOsO_6$ are closely located in energy (Fig. 5). This gives rise to a strong hybridization between the majority spin V t_{2g} and minority spin Os t_{2g} orbitals via O p_π orbitals which results in the broad B and B' t_{2g} hybridized spin down conduction band in the energy range of $-2.0-1.0$ eV, and further strengthens the AFM exchange coupling between the V and Os ions. Clearly, this coupling between the V and Os t_{2g} orbitals via O p_π orbitals would allow the spin-down conduction electrons to hop freely from a V ion to the neighboring Os ions and back to the V ion, resulting in a lower kinetic energy. This situation is similar to the double exchange mechanism[28] of the metallic ferromagnetism in the colossal magnetoresistive manganites, and hence may be called the generalized double exchange mechanism. The direct on-site exchange interaction would then lower the majority spin Os t_{2g} band below E_F and push the minority spin V t_{2g} band above E_F, thereby creating an insulating gap in the spin up channel (see Fig. 5). As a result, the band gap may be called an antiferromagnetic coupling gap.[7] Therefore the antiferromagnetism in $LaSrVOsO_6$ has the dominant contributions from both the superexchange mechanism and the generalized double exchange mechanism (see Refs. 29 and 30 for the detailed analysis on these two mechanisms in the doped ferromagnetic manganites). The origin of the half-metallicity is essentially the same as that of the HM ferrimagnetic double perovskites such as Sr_2FeMoO_6, namely, the $B(t_{2g})$-O$(2p_\pi)$-$B(t_{2g})$ hybridization, as illustrated in Refs. 7 and 23. It could then be inferred from this discussion that the antiferromagnetic transition temperature T_N in the HM-AFMs would be in the same order of magnitude as that in Sr_2FeMoO_6 (T_c=419 K),[5] i.e., being above room temperature.

The electronic structures of $LaSrMoTcO_6$ and $LaSrMoReO_6$ are similar to that of $LaSrVOsO_6$, as can be seen from Figs. 5–7. In particular, the electronic structure of $LaSrMoTcO_6$ is nearly identical to that of $LaSrVOsO_6$. The discernible difference in the electronic structure between $LaSrMoTcO_6$ and $LaSrVOsO_6$ is the larger Mo 4d contribution to the O 2p dominant lower valence band, indicating a stronger Mo 4d-O 2p bonding in $LaSrMoTcO_6$. This may be expected because the Mo 4d orbitals are significantly more extended than that of V 3d. There are also some discernible differences in the electronic structure between $LaSrMoReO_6$ and $LaSrVOsO_6$. The most pronounced difference is that there is a small dip or pseudogap at E_F in the spin-down channel. Therefore the spin-down band structure of $LaSrMoReO_6$ may be regarded as a semimetal with a small DOS of 0.6 states/eV/spin/f.u. at E_F. The spin-down DOS at E_F further decreases when Sr is replaced by Ba (see Table VII). Further differences among the electronic structures of $LaSrVOsO_6$, $LaSrMoTcO_6$, and $LaSrMoReO_6$ are minor and they include slight differences in the energy position and bandwidth of various bands.

TABLE VIII. Calculated structural parameters, magnetic and electronic properties of antiferromagnetic insulators LaACrYO$_6$ in theoretically determined P4/nmm structures.

A=		Ca	Sr	Ba
		(a) LaACrTcO$_6$		
a (Å)		5.534	5.573	5.638
c/a		1.4123	1.4117	1.4068
V (Å^3/f.u.)		119.66	122.20	126.08
m_{Cr} (μ_B)		−2.241	−2.264	−2.295
m_{Tc} (μ_B)		1.683	1.696	1.710
m_t (μ_B/f.u.)		0.0	0.0	0.0
gap (eV)	↑	1.252	1.224	1.197
	↓	0.653	0.680	0.762
		(b) LaACrReO$_6$		
a (Å)		5.551	5.583	5.650
c/a		1.4117	1.4111	1.4070
V (Å^3/f.u.)		120.72	122.79	126.89
m_{Cr} (μ_B)		−2.217	−2.237	−2.271
m_{Tc} (μ_B)		1.468	1.484	1.503
m_t (μ_B/f.u.)		0.0	0.0	0.0
gap (eV)	↑	0.63	0.76	0.85
	↓	0.98	1.09	1.12

D. Unconventional antiferromagnetic insulators

In our first round of search for the HM-AFMs, we also found LaACrTcO$_6$ and LaACrReO$_6$ to be antiferromagnets. However, LaACrTcO$_6$ and LaACrReO$_6$ are insulators. Nonetheless, we may regard these materials as unconventional AFM insulators because they have several subtle differences in the electronic structure from archetypical AFM insulators such as MnO and NiO in the cubic rocksalt structure. The calculated electronic and magnetic properties of these materials are listed in Table VIII. The total and orbital-decomposed DOS spectra of LaSrCrTcO$_6$ are displayed in Fig. 8, as an example. These results are obtained from self-consistent electronic structure calculations for the fully theoretically optimized crystal structures. Compared with the HM-AFMs, these compounds have a stronger spin splitting of the $B(B')$ t_{2g} band and a larger local magnetic moment on the B and B' sites (see Fig. 8 and Table VIII). For instance, the spin splitting of the Cr t_{2g} band in LaSrCrTcO$_6$ is about 2.5 eV, significantly larger than that of the V t_{2g} band of less than 1.5 eV in LaSrVOsO$_6$. The local magnetic moment on the Cr site in LaACrTc(Re)O$_6$ is twice as large as that on the V site in LaAVOsO$_6$. Furthermore, the spin-down Cr t_{2g} band in LaACrTc(Re)O$_6$ is aligned with the spin-up Tc(Re) t_{2g} band, rather than with the spin-down Tc(Re) t_{2g} band as is the case in the HM-AFM compounds discussed in the previous section. Consequently, in LaATc(Re)O$_6$, the generalized double exchange mechanism is ineffective and the antiferromagnetic coupling is due solely to the traditional superexchange mechanism. This gives rise to the AFM insulating behavior in these compounds.

In the conventional AFM insulators, the two antiferromagnetic coupled ions are made of the same atomic species, e.g., Ni in NiO. The two spin-decomposed total DOS spectra are identical and the insulating gaps for spin-up and spin-down channels are the same. The features of the present AFM insulators include that the two spin-decomposed total DOS spectra are no longer the same and the spin-up insulating gap may have a size different from that of the spin-down insulating gap, as shown in Table VIII and Fig. 8, and that the antiferromagnetic coupled ions consist of two different atomic species, e.g., Cr and Tc in LaACrTcO$_6$.

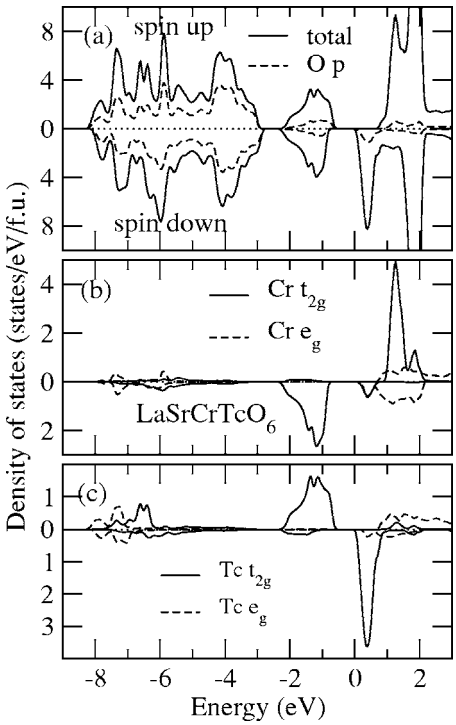

FIG. 8. Total and orbital-decomposed density of states of LaSrCrTcO$_6$ in the theoretically determined P4/nmm structure.

V. CONCLUSIONS

In conclusion, in order to search for the fascinating half-metallic antiferromagnetic materials, we have carried out a systematic *ab initio* study of the ordered double perovskites LaABB'O$_6$ with the possible B and B' pairs from all the 3d, 4d, and 5d transition metal elements being considered. Electronic structure calculations based on first-principles density-functional theory with GGA for more than 60 double perovskites LaCaBB'O$_6$ have been performed using the all-electron FLAPW method. As a result, we find three families of the HM-AFMs, namely, LaAVOsO$_6$, LaAMoTcO$_6$, and LaAMoReO$_6$ (A=Ca,Sr,Ba). The found HM-AFM state in these materials subsequently survives the full *ab initio* lattice constant and atomic position optimizations which were carried out using the frozen-core full potential PAW method. We attribute the AFM to both the superexchange mechanism and the generalized double exchange mechanism via the $B(t_{2g})$-O$(2p_\pi)$-$B'(t_{2g})$ coupling and also believe the latter to be the origin of the HM. We also find that the HM-AFM properties predicted previously in some of the double perovskites

would disappear after the full structural optimizations, thereby providing an explanation why the previous experimental attempts to synthesize the HM-AFM double perovskites did not succeed. Finally, in our search for the HM-AFMs, we find La*A*CrTcO_6 and La*A*CrReO_6 to be AFM insulators of an unconventional type in the sense that the two antiferromagnetic coupled ions consist of two different elements and that the two spin-resolved densities of states are no longer the same. Stimulated by previous theoretical predictions of the HM-AFM in La_2MnVO_6 (Ref. 11) and also in La*A*VRuO_6, (Ref. 13), experimental effort to synthesize the HM-AFMs has been reported by Androulakis *et al.*[14] and attempted by Liu *et al.*,[24] respectively, which were, however, unsuccessful. It is hoped that our predictions of robust HM-AFMs would encourage further experimental searches for the HM-AFMs.

ACKNOWLEDGMENTS

The authors thank Ru Shi Liu for helpful discussions on the possibility of synthesis of the half-metallic antiferromagnet double perovskites. The authors gratefully acknowledge financial support from National Science Council of Taiwan and NCTS/TPE. They also thank the National Center for High-Performance Computing of Taiwan for providing CPU time.

*Electronic address: gyguo@phys.ntu.edu.tw

[1] R. A. de Groot, F. M. Müeller, P. G. van Engen, and K. H. J. Buschow, Phys. Rev. Lett. **50**, 2024 (1983).
[2] A. Yanase and K. Siratori, J. Phys. Soc. Jpn. **53**, 312 (1984).
[3] K. Schwarz, J. Phys. F: Met. Phys. **16**, L211 (1986).
[4] J.-H. Park, E. Vescovo, H.-J. Kim, C. Kwon, R. Ramesh, and T. Venkatesan, Nature (London) **392**, 794 (1998).
[5] K.-I. Kobayashi, T. Kimura, H. Sawada, K. Terakura, and Y. Tokura, Nature (London) **395**, 677 (1998).
[6] W. E. Pickett and J. S. Moodera, Phys. Today **54**, 39 (2001).
[7] H.-T. Jeng and G. Y. Guo, Phys. Rev. B **67**, 094438 (2003).
[8] H. van Leuken and R. A. de Groot, Phys. Rev. Lett. **74**, 1171 (1995).
[9] W. E. Pickett, Phys. Rev. Lett. **77**, 3185 (1996).
[10] R. E. Rudd and W. E. Pickett, Phys. Rev. B **57**, 557 (1998).
[11] W. E. Pickett, Phys. Rev. B **57**, 10613 (1998).
[12] M. S. Park, S. K. Kwon, and B. I. Min, Phys. Rev. B **64**, 100403(R) (2001).
[13] J. H. Park, S. K. Kwon, and B. I. Min, Phys. Rev. B **65**, 174401 (2002).
[14] J. Androulakis, N. Katsarakis, and J. Giapintzakis, Solid State Commun. **124**, 77 (2002).
[15] P. Hohenberg and W. Kohn, Phys. Rev. **136**, B864 (1964); W. Kohn and L. J. Sham, Phys. Rev. **140**, A1133 (1965).
[16] J. P. Perdew, K. Burke, and M. Ernzerhof, Phys. Rev. Lett. **77**, 3865 (1996).
[17] O. K. Andersen, Phys. Rev. B **12**, 3060 (1975).
[18] D. D. Koelling and G. O. Arbman, J. Phys. F: Met. Phys. **5**, 2041 (1975).
[19] P. Blaha, K. Schwarz, G. K. H. Madsen, D. Kvasnicka, and J. Luitz, WIEN2K, An Augmented Plane Wave1 Local Orbitals Program for Calculating Crystal Properties (Techn. University Wien, Austria, 2002).
[20] P. E. Blöchl, O. Jepsen, and O. K. Andersen, Phys. Rev. B **49**, 16223 (1994).
[21] P. E. Blöchl, Phys. Rev. B **50**, 17953 (1994); G. Kresse and D. Joubert, *ibid.* **59**, 1758 (1999).
[22] G. Kresse, and J. Hafner, Phys. Rev. B **48**, 13115 (1993); G. Kresse and J. Furthmüller, Comput. Mater. Sci. **6**, 15 (1996); Phys. Rev. B **54**, 11169 (1996).
[23] H. Wu, Phys. Rev. B **64**, 125126 (2001).
[24] R. S. Liu (private communication).
[25] H. L. Skriver, *The LMTO Method* (Springer-Verlag, Berlin, 1984), Tables 10.1 and 10.2.
[26] Note that if there are high peaks on both sides of the Fermi level and the intra-atomic exchange interaction is sufficiently strong, the system might transit to a high spin magnetic state (Ref. 27) even though the standard Stoner criterion is not fulfilled. Nevertheless, since the intra-atomic exchange interaction for both the V and Ru atoms is only moderate [see, e.g., J. F. Janak, Phys. Rev. B **16**, 255 (1977)], we believe that this metamagnetic transition would not occur in La*A*VRuO_6, as our explicit spin-polarized calculations have shown.
[27] M. Cyrot and M. Lavagna, J. Phys. (Paris) **40**, 763 (1979).
[28] C. Zener, Phys. Rev. **82**, 403 (1951).
[29] I. V. Solovyev and K. Terakura, Phys. Rev. Lett. **82**, 2959 (1999).
[30] I. V. Solovyev, and K. Terakura, in *Electronic Structure and Magnetism of Complex Materials*, edited by D. J. Singh and D. A. Papaconstantopoulos (Springer-Verlag, Berlin, 2003).